Molecular Biology of the Cell
Vol. 10, 1511–1520, May 1999

Radixin Is Involved in Lamellipodial Stability during Nerve Growth Cone Motility

Leslie Castelo and Daniel G. Jay*

Department of Physiology, Tufts University School of Medicine, Boston, Massachusetts 02111

Submitted November 16, 1998; Accepted February 17, 1999.
Monitoring Editor: Martin Raff

Immunocytochemistry and in vitro studies have suggested that the ERM (ezrin-radixin-moesin) protein, radixin, may have a role in nerve growth cone motility. We tested the in situ role of radixin in chick dorsal root ganglion growth cones by observing the effects of its localized and acute inactivation. Microscale chromophore-assisted laser inactivation (micro-CALI) of radixin in growth cones causes a 30% reduction of lamellipodial area within the irradiated region whereas all control treatments did not affect lamellipodia. Micro-CALI of radixin targeted to the middle of the leading edge often split growth cones to form two smaller growth cones during continued forward movement (>80%). These findings suggest a critical role for radixin in growth cone lamellipodia that is similar to ezrin function in pseudopodia of transformed fibroblasts. They are consistent with radixin linking actin filaments to each other or to the membrane during motility.

INTRODUCTION

The nerve growth cone is the sensory motile organelle that translates extracellular cues into axon guidance via directed motility (reviewed by Tanaka and Sabry, 1995; Jay, 1996). They do so by localized changes in motility at the leading edge that bias the movement of the rest of the growth cone (Jay, 1996). It is clear from studies in vitro (Marsh and Letourneau, 1984) and in vivo (Bentley and Toroian-Raymond, 1986) that F-actin is critical for directing growth cone motility. Specific actin-associated proteins are required to control F-actin at the leading edge, but it has been difficult to show which of the many actin-associated proteins act at that location (Letourneau, 1996).

Among the best candidates to act at the leading edge of the growth cone is radixin (Gonzalez-Agosti and Solomon, 1996). Radixin is a prototypic member of the ERM (ezrin-radixin-moesin) family of proteins (reviewed by Arpin *et al.*, 1994; Tsukita *et al.*, 1997). It was initially identified as a barbed end capping protein (Tsukita *et al.*, 1989) and was later shown to be highly homologous to ezrin and moesin (Funayama *et al.*, 1991; Sato *et al.*, 1991). Cryptic F-actin–binding sites within the carboxyl-terminal domain were revealed by denaturation studies and by expression of single domains of radixin in vitro (Henry *et al.*, 1995; Magendantz *et al.*, 1995). Similar sites have also been seen with ezrin and moesin (Gary and Bretscher, 1993; Turunen *et al.*, 1994; Martin *et al.*, 1995). Radixin and other ERM proteins also bind to membrane proteins such as CD44 that, in turn, can bind to hyaluronic acid in the extracellular matrix (Tsukita *et al.*, 1994). From these studies, it has been hypothesized that the ERM proteins work as plasma membrane–actin filament cross-linkers (Algrain *et al.*, 1993; Tsukita *et al.*, 1994). Radixin is the predominant ERM family member in chick sympathetic neuronal growth cones, and its localization is diminished after induction of growth cone collapse (Gonzalez-Agosti and Solomon, 1996). Together, these studies suggest that radixin has a role in growth cone shape and motility but, thus far, direct evidence to support this hypothesis has been lacking.

It has been difficult to show that any specific ERM protein functions in cells. ERM proteins are highly homologous with each other and are often coexpressed (Sato *et al.*, 1991). They colocalize and bind to similar sites (Henry *et al.*, 1995) and may have overlapping functions (Takeuchi *et al.*, 1994). Overexpression (Henry *et al.*, 1995) and misexpression (Martin *et al.*, 1995) of radixin or ezrin domains cause cell shape changes, but these studies have not shown specific roles for any one of the ERM proteins. Reduction of all three ERM proteins by antisense oligonucleotide ex-

* Corresponding author. E-mail address: djay01@emerald.tufts.edu.

pression showed defects in cell attachment of mouse epithelial cells, but antisense expression of any one ERM protein had little effect (Takeuchi *et al.*, 1994). These experiments did, however, suggest a more specific role for moesin in microvilli formation in thymoma cells (Takeuchi *et al.*, 1994).

Recently, essential roles for ezrin were shown using microscale chromophore-assisted laser inactivation (micro-CALI) to inactivate ezrin in fibroblasts (Lamb *et al.*, 1997). Micro-CALI inactivates a protein within a 10-μm region by targeting a 620-nm laser microbeam via a specific antibody that is labeled with the dye Malachite green (MG) (Jay, 1988; Diamond *et al.*, 1993). The acute and localized inactivation of ezrin resulted in a loss of membrane ruffling and pseudopodial retraction in transformed fibroblasts, and in marked retraction of the leading edge of normal fibroblasts. This study suggests that ezrin has critical roles in fibroblast cell shape and motility (Lamb *et al.*, 1997). It also suggests that a similar strategy would be useful to address the role of radixin in growth cone shape and motility. In the present study, we applied micro-CALI to show a role for radixin in embryonic chick dorsal root ganglion (DRG) neuronal growth cones.

MATERIALS AND METHODS

Chick DRG Neuronal Culture

Dissociated chick DRG neurons were prepared as described by Sydor *et al.* (1996). DRGs were dissected from E10–12 chick embryos and suspended in 0.25% trypsin in HBSS for 8 min. After trypsinization, cells were spun down at 1000 $\times$ *g* for 2 min, and the cell pellet was resuspended in chick neuronal media (L-15 media from Sigma Chemical, St. Louis, MO, supplemented with 10% fetal bovine serum from Hyclone, Logan UT). Cells were triturated using an up-and-down motion of a 200-μl Gilson Pipetteman, set at 40 μl (~80 gentle strokes). They were then plated on donut dishes (30-mm culture dishes with 11/16 in. drill holes affixed with coverslips coated with poly-L-lysine and laminin) with 3 ml of chick neuronal media. Cells were incubated at 37°C in an air incubator for 1.5–2 h before experimentation.

Antibodies

Affinity-purified anti-radixin antibodies were generous gifts of Frank Solomon and Etchell Cordero (Massachusetts Institute of Technology, Cambridge, MA) and have been previously described by Winckler *et al.* (1994). Rabbit polyclonal antibody 457–3 is specific for radixin alone and was raised against amino acids 400–409 in the carboxyl-terminal domain of radixin. Rabbit polyclonal antibody 220, which recognizes ezrin, radixin, and moesin, was raised against the first 13 amino acids at the amino terminus that are common to all three ERM proteins. We used the following secondary antibodies (from Cappel Laboratories, Malvern PA): rhodamine- or fluorescein-conjugated goat anti-rabbit IgG; and fluorescein-conjugated rabbit anti-mouse IgG. For micro-CALI experiments, antibodies were labeled with MG as previously described by Beermann and Jay (1994). Labeling ratios of MG-457–3, MG-220, and MG-IgG were ~6–8 dye moieties/IgG molecule.

Antibody Loading

For both micro-CALI and immunocytochemistry experiments, neurons were loaded via trituration with MG-labeled or unlabeled primary antibodies as described by Sydor *et al.* (1996). After trypsinization, antibody solutions (50 μl) at 2 mg/ml in HBSS with 1 mg/ml fluorescein-labeled IgG (as a tracer) were added to six whole DRGs during trituration. After trituration, cells were separated by 2 min of centrifugation at 1000 $\times$ *g*. The antibody solution was removed and cells were gently resuspended in chick neuronal media before plating. Trituration creates temporary holes in the cell membrane, enabling antibodies to enter (Borasio *et al.*, 1989) and has been used to load antibodies for micro-CALI previously (Chang *et al.*, 1995; Sydor *et al.*, 1996).

Immunocytochemistry

Cultured chick DRG neurons on glass coverslips were fixed with 3.7% paraformaldehyde in PBS for 25 min at 37°C, washed three times with PBS, permeabilized by 0.05% Triton X-100/PBS for 15 min at room temperature, and blocked with 10% fetal calf serum in PBS for 30 min. Fixed neurons were incubated overnight in primary antibodies (1:500 dilution of 457–3; 1:1000 for 220), washed extensively, and then probed with rhodamine- or FITC-conjugated secondary antibodies (1:100, diluted in blocking buffer) for 2 h at room temperature. After five 10-min rinses in PBS, coverslips were mounted in Fluoromount-G (Southern Biotechnology Associates) and were then viewed with a Zeiss confocal microscope (model LSM 410; Carl Zeiss, Thornwood, NY).

Immunoblotting

Immunoblot analysis was performed according to Dubreil *et al.* (1987). In brief, chick DRGs were collected and placed in 200 μl of HBSS (without calcium or magnesium) and spun down briefly at 1000 $\times$ *g*. HBSS was removed, and 2% boiling SDS sample buffer was added. The sample was then boiled for 3 min, sonicated at 70% duty cycle for 3 min, and boiled for an additional 5 min. DRG lysates (4 DRGs per lane) were separated by electrophoresis on 7.5% SDS-PAGE minigels and transferred by electrophoresis to nitrocellulose at 40 V for 1.5 h. Nitrocellulose blots were then blocked with 5% nonfat dry milk in 0.03% Triton X-100 in PBS for 1.5 h at room temperature. They were incubated for 2.5 h at room temperature with 457–3 (1:500) and 220 (1:1000) and probed with alkaline phosphatase-labeled goat anti-rabbit IgG antibodies (1:500) for 1 h at room temperature. Blots were then developed in alkaline phosphatase substrate (Sigma Chemical, St. Louis MO).

Micro-CALI of Proteins in Growth Cones

Micro-CALI was performed on chick DRG growth cones 1–6 h after plating according to Wang *et al.* (1996). Throughout the micro-CALI experiments, DRG cultures were maintained at 37°C with a stage incubator (Opti-Quip, Highland Mills, NY). In a typical micro-CALI experiment, antibody-loaded neurons were selected by epifluorescence. A selected growth cone was observed by video-enhanced time-lapse microscopy (Scion Image software) for 5 min (recorded every 15 s) as described by Wang *et al.* (1996). A region of the growth cone was laser irradiated for 5 min using a nitrogen-driven pulsed dye laser (model 337, Laser Science, Newton MA) with the fluorescent laser dye DCM and observed for an additional 10 min.

Methods of Quantitation

Results of asymmetrical (half-growth cone) micro-CALI studies were measured using NIH Scion System Software. Lamellipodial area was measured in every frame of the time-lapse period and plotted as a function of time. The rates of retraction were obtained by taking the first derivative of these plots. Area retraction was defined as a percent decrease in the lamellipodial area (μm^2) in laser-irradiated or unirradiated regions during 5 min of observation. The rates of lamellipodial retraction/extension and the percent change in lamellipodial surface area inside and outside the irradiated region were compared 5 min before irradiation to ensure that

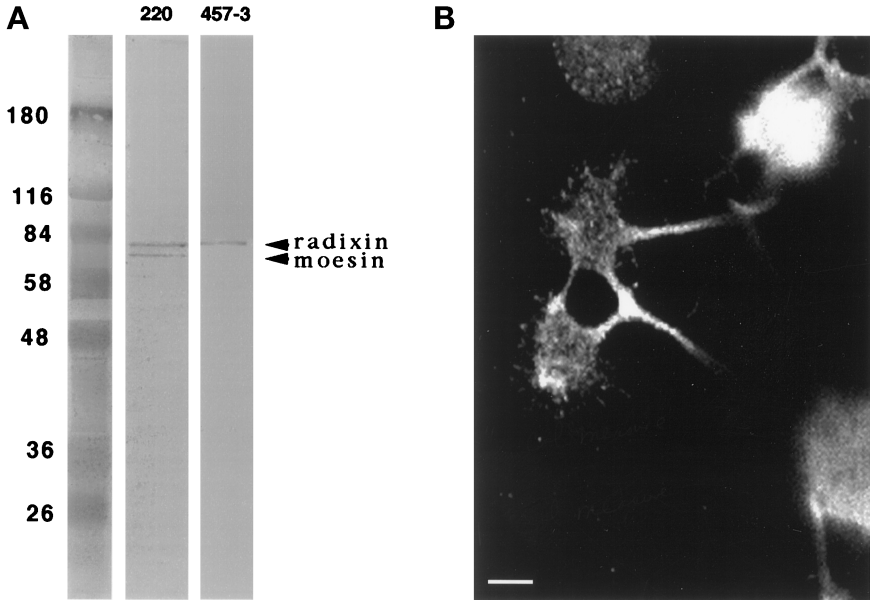

Figure 1. Specificity of anti-radixin antibodies. (A) DRG neuronal lysates analyzed by immunoblot with rabbit polyclonal antibodies 220 (lane a) and 457–3 (lane b). Antibody 457–3 (which is specific for radixin) recognizes a single band corresponding to radixin. Antibody 220 (which binds to all three ERM proteins) recognizes two bands with molecular weights corresponding to radixin and moesin. DRG neuronal lysates do not appear to express ezrin. (B) DRG-dissociated neurons were grown on laminin-poly-L-lysine–coated coverslips and were fixed and probed with 457–3 anti-radixin followed by FITC-labeled anti-rabbit IgG. Radixin is present throughout the growth cone and exhibits a punctate pattern. Staining was undetectable for controls that lack 457–3.

they were statistically indistinguishable. Additionally, neurite length was measured before, during, and after laser irradiation using NIH Scion Imaging software. A fixed point on the base of the cell body was chosen as a landmark at t = 0 min. All subsequent measurements began at this fixed point and ended at the base of the growth cone body. Neurite extension rate was defined as the change in neurite length (μm/min) during the period of time-lapse observation. Results of symmetrical growth cone studies were scored as splitting versus not splitting after micro-CALI. A split growth cone was defined as a growth cone whose laser-irradiated region retracted but whose unirradiated regions continued to grow and diverge into two smaller growth cones.

All quantitative data are reported as mean ± SD. These data were obtained from more than 10 experiments and a total of more than 20 growth cones for each experimental condition. Statistical analysis was performed with Stat View II (Abacus Concept, Berkeley, CA). Analysis of the significance between percent change of lamellipodial area was assessed using Student's two-tailed, paired *t* test for asymmetric application of micro-CALI, and unpaired *t* test for comparison between samples using MG-labeled nonimmune IgG- and Mg-labeled anti-radixin–loaded growth cones for micro-CALI. Analysis of variance and Poisson test were also used to assess significance between multiple sets of data.

RESULTS

The hypothesis that radixin has a critical role in growth cone motility (Gonzalez-Agosti and Solomon, 1996) was tested in DRG neuronal growth cones in culture using micro-CALI. This approach allowed us to observe changes in growth cone morphology and motility in response to the acute and localized loss of radixin. To perform micro-CALI, a specific antibody is tagged with MG dye, which is then introduced into DRG neurons by trituration, and the neurons are allowed to extend neurites in culture. An area of inactivation within the growth cone is selected, and irradiated with a laser microbeam at a wavelength of 620 nm. The MG label absorbs this laser light to generate short-lived free radicals (Liao *et al.*, 1994) that selectively inactivate proteins bound by the MG-labeled antibody. CALI takes advantage of the specificity inherent in tight binding interactions, as unbound MG-labeled reagents do not cause significant damage (reviewed by Wang and Jay, 1996).

Specificity of Antibodies

For these studies we employed two polyclonal antibodies: 457–3, which recognizes the carboxyl-terminal domain of radixin alone (Winckler *et al.*, 1994); and 220, which recognizes the amino terminus of all three ERM proteins. We tested their specificity by immunoblot analysis and immunocytochemistry. Immunoblotting confirmed that 457–3 and 220 specifically recognized ERM species in DRG neuronal lysates (Figure 1A). Immunoblotting of DRG cell lysates with 457–3 detected a predominant 82 kDa species, which corresponds to the molecular mass of radixin. Immunoblotting of DRG cell lysates with 220 showed two bands of similar intensity at 82 kDa and 75 kDa, which correspond to the apparent molecular weights of radixin and moesin, respectively. It is possible that the moesin comes from contaminating fibroblasts in the lysate, even though DRGs have many more neurons than fibroblasts. This is unlikely because a band corresponding to ezrin (85 kDa), which is abundant in fibroblasts (Lamb *et al.*, 1997), was not detected in these immunoblots. The lack of this band shows that fibroblast contamination was small and suggests that moesin is present in DRG neurons.

Immunocytochemistry with 457–3 was used previously to show the presence of radixin in the chick

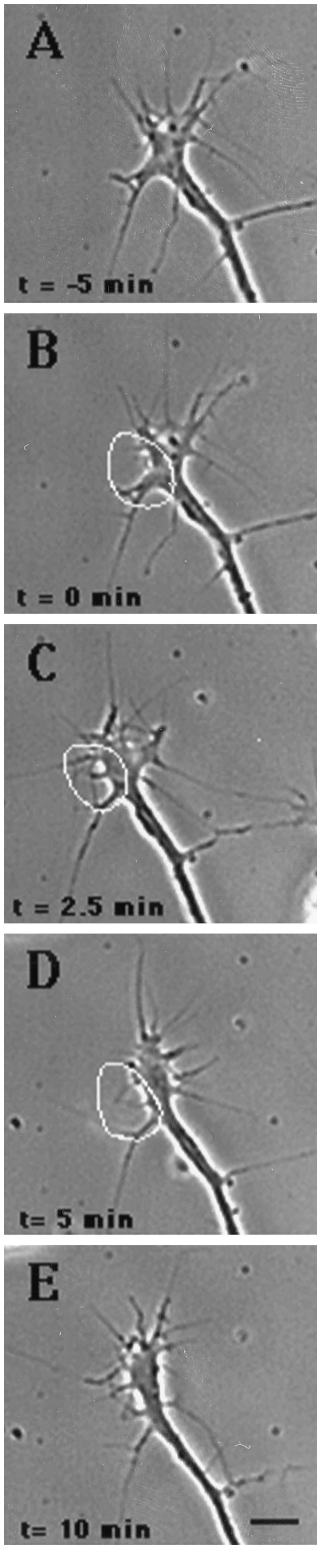

Figure 2. Micro-CALI of radixin causes lamellipodial retraction. A chick DRG neuron was loaded with MG-labeled 457–3 and plated on a laminin-coated coverslip to allow a growth cone to emerge and time-lapse imaging was begun at t = −5 min (A). The growth cone was subjected to laser irradiation on one side of the growth cone (white circle) beginning at t = 0 min (B) and ending at t = 5 min (C), and the growth cone was observed for another 10 min (D and E). The lamellipodia in the irradiated half retracts (B–D) and begins to recover by t = 10 min (E). Scale bar, 10 μm.

sympathetic neurons (Gonzalez-Agosti and Solomon, 1996). We used this assay to show that radixin is also found in the growth cones of chick DRG neurons (Figure 1B). Growth cones were brightly stained, as were cell bodies and neurites. Within the growth cone, radixin staining was uniform and exhibited a punctate pattern (Figure 1B) that extended out from the lamellipodia into the filopodia. This pattern was similar to the staining observed with two other anti-ERM antibodies previously reported: 904, which recognizes all ERM isoforms (Birgbauer *et al.*, 1991); and 3D11, which recognizes radixin (Everett and Nichol, 1990). Immunocytochemistry with 220 showed similar but heavier staining throughout the growth cone, cell body, and neurites (data not shown) most likely reflecting the ability of this antibody to recognize both radixin and moesin in DRG neurons. The pattern observed was different than that seen using 13H9 with DRG neurons; this antibody brightly stained filopodia (Goslin *et al.*, 1989; Birgbauer *et al.*, 1991). While 13H9 detects an ezrin-like immunoreactivity, it does not recognize ERM proteins by immunoblot (Gonzalez-Agosti, personal communication).

Together, these experiments show that 457–3 and 220 have the specificity required for their use for micro-CALI of radixin in DRG growth cones. As no other bands are detected by immunoblotting using 457–3, this antibody is unlikely to bind to other proteins in DRG neurons. Thus, the effects of micro-CALI using 457–3 would be specific for radixin. Micro-CALI using 220 would be expected to inactivate both radixin and moesin in DRG neurons. The use of 457–3 and 220 for micro-CALI also allows us to target two different domains of radixin.

Micro-CALI of Radixin Causes Lamellipodial Retraction

Micro-CALI of radixin using MG 457–3 resulted in a rapid lamellipodial retraction of the irradiated half. Figure 2 shows an example of this. There was a marked retraction of lamellipodia in the irradiated half during the laser period, t = 0–5 min, but no retraction of the unirradiated half (Figure 2, B–D). Filopodia did not appear to be affected. They maintained their structure throughout this period of lamellipodial retraction. The growth cone pictured in Figure 2 showed a turning away from the irradiated region but this is not always so. The asymmetric loss of radixin may direct subsequent neurite outgrowth, but recovery is rapid (see below), and a short period of

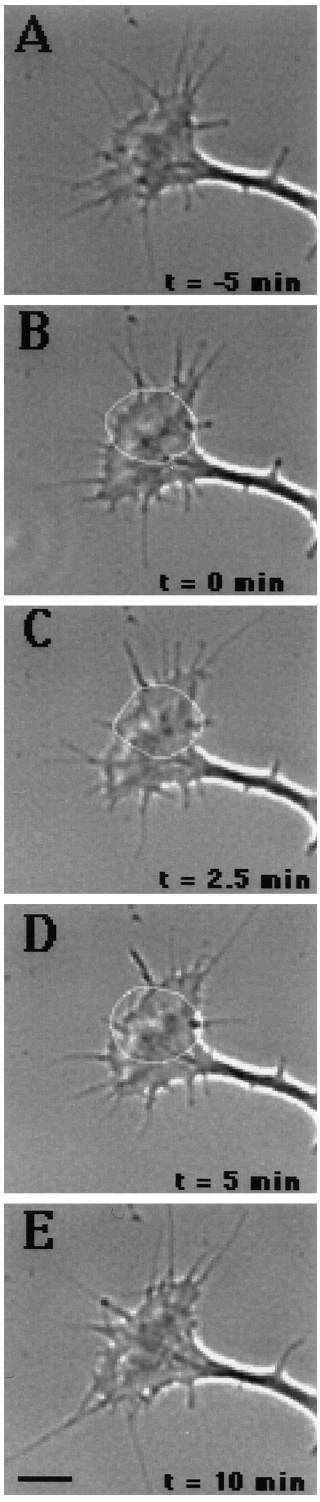

Figure 3. Micro-CALI using MG-nonimmune IgG has no effect. A chick DRG neuron was loaded with MG-labeled nonimmune IgG and plated on laminin-coated coverslip to allow a growth cone to emerge. Time-lapse imaging was begun at t = −5 min (A). The growth cone was subjected to laser irradiation within a small region of the growth cone (white circle) beginning at t = 0 min (B) and ending at t = 5 min (C), and the growth cone was observed for another 10 min (D and E). The lamellipodia within the irradiated region do not retract (B–E). Scale bar, 10 μm.

loss of function may not be sufficient to cause turning. Indeed, the localized inactivation of myosin Iβ must be performed several times to evoke turning (Wang and Jay, unpublished data).

In contrast, laser irradiation of growth cones loaded with dye-labeled nonimmune IgG (MG IgG) had no effect on lamellipodial area (Figure 3). Normal growth continued and normal growth cone morphology was maintained throughout the growth cone (Table 1). There was no observable difference between irradiated and nonirradiated sides of the growth cone. Loading of MG-labeled anti-radixin antibodies also did not affect lamellipodia by themselves. The changes of lamellipodial area for growth cones loaded with MG-anti-radixin or MG-nonimmune IgG were indistinguishable without laser irradiation (Table 1, Prelaser and Postlaser). This shows that the MG-457–3 by itself did not affect function with respect to growth cone motility (although other roles of radixin may have been affected).

Table 1 shows the quantitation of lamellipodial retraction caused by micro-CALI of radixin or by irradiation of MG-labeled nonimmune-IgG-loaded neurons. In general, lamellipodia extend and retract over time such that there is no net average change in lamellipodial area. This was observed for all control treatments, and these values range from ~−1.5 to 2% of the initial lamellipodial area. These values are statistically indistinguishable from each other ($p > 0.2$). In contrast, regions of DRG growth cones treated with micro-CALI of radixin showed a ~30% decrease in lamellipodial area within the laser spot. This decrease was significantly different than lamellipodial change on the unirradiated sides of growth cones ($n = 24$, $p < 0.0001$ by paired *t* test) and was also significantly different from all control treatments ($p < 0.0001$ by analysis of variance).

These experiments showed that binding of the MG-457–3 to radixin together with laser irradiation was responsible for the lamellipodial retraction observed. Irradiation of growth cones loaded with MG-nonimmune antibodies also had no effect on lamellipodia. Importantly, there was no significant difference between the irradiated and nonirradiated regions of micro-CALI-treated growth cones before or after laser irradiation. That there was no significant difference before laser irradiation shows that there was no bias in selecting regions to be irradiated. That there was no significant difference after laser irradiation shows that growth cones recover rapidly, likely due to the move-

Figure 3 (cont). ending at t = 5 min (C), and the growth cone was observed for another 10 min (D and E). The lamellipodia within the irradiated region do not retract (B–E). Scale bar, 10 μm.qending at t = 5 min (C), and the growth cone was observed for another 10 min (D and E). The lamellipodia within the irradiated region do not retract (B–E). Scale bar, 10 μm.

Table 1. Micro-CALI of radixin causes lamellipodial retraction half-growth cone studies

	% Change of lamellipodial surface area over time ± SEM					
	Prelaser		During laser		Postlaser	
Treatment	Unirradiated half	Irradiated half	Unirradiated half	Irradiated half	Unirradiated half	Irradiated half
MG-IgG loaded cells (n = 22)	0.55% ± 0.65	−0.60% ± 0.81	0.51% ± 0.61	0.71% ± 0.82	1.24% ± 0.96	−0.33% ± 0.85
MG-457-3 loaded cells (n = 25)	0.28% ± 1.12	0.24% ± 1.21	−1.48% ± 1.72	−30.48% ± 2.47[a]	0.39% ± 1.20	2.14% ± 1.01

Percent change of lamellipodial surface area was measured for irradiated and nonirradiated halves of MG IgG (control) and MG 457-3 growth cones over 5 min. As lamellipodia extend and retract over time, the average percent change for untreated growth cones is close to 0% (0.35% ± 0.74, n = 11). Significance was measured by Student's two-tailed, paired, *t* test.

[a] $p < 0.0001$.

ment of active radixin from unirradiated regions. Together these data show that micro-CALI of radixin causes lamellipodial retraction in neuronal growth cones.

Micro-CALI of Radixin Causes Growth Cone Splitting

When micro-CALI of radixin was directed to the middle of the leading edge, growth cones often split (Figure 4). The leading edge retracted while the unirradiated regions grew and extended normally. Continued motility divided the growth cone into two separate growth cones (Figure 4, D and E) each with a nascent neurite. The time course of growth cone splitting after micro-CALI was rapid with a $t_{1/2}$ of ~2 min (Figure 5). Although growth cone splitting can occur spontaneously in vivo (Letourneau *et al.*, 1986), in these experiments, it occurred precisely during laser irradiation, suggesting that it was a direct result of micro-CALI of radixin. Table 2 shows the percentage of growth cones that split for every experimental and control condition. More than 80% of the growth cones showed splitting during irradiation of MG 457–3-loaded neurons. This splitting frequency was significantly different than that observed for all control treatments ($p < 0.0001$ by Poisson test). In contrast, only one growth cone during laser irradiation in a population of cells loaded with MG IgG (4.5%; $p > 0.5$ by Poisson test). Splitting was also strictly dependent on the dye-labeled antibody. Untreated cells, cells loaded with unlabeled 457–3 and 220, or cells loaded with MG-nonimmune IgG showed no splitting regardless of laser light.

Micro-CALI of Radixin Using Two Different Antibodies Has Similar Effects

Thus far, micro-CALI has been directed to radixin via 457–3, which recognizes the carboxyl-terminal domain of radixin specifically (Winckler *et al.*, 1994). To further test our hypothesis of radixin function, we applied micro-CALI using MG-labeled 220, which binds to radixin at its amino terminus. The effects of micro-CALI using MG-labeled 220 were indistinguishable from those observed after micro-CALI using MG-labeled 457–3 (Table 2). The time course of growth cone splitting is also indistinguishable for these two samples (Figure 5). No additional changes in growth cone behavior were seen using MG-labeled 220 for micro-CALI. Thus, micro-CALI, using two different antibodies that bind to different domains of the radixin polypeptide, causes similar effects on growth cone behavior. These findings suggest that the effects of micro-CALI are specific and support the hypothesis that radixin is involved in lamellipodial stability. However, it is also possible that the amino- and carboxyl-termini are close together in radixin's three-dimensional structure, and it has been suggested that they associate in native radixin (Magendantz *et al.*, 1995).

The 220 antibody also binds to ezrin and moesin, and moesin is also present in DRG neurons (Figure 1A). As such, if moesin had a different role in growth cone motility, we might have expected to see different growth cone behaviors in response to micro-CALI using MG-labeled 220. We did not see this. This suggests that disruption of radixin is sufficient to cause growth cone splitting and that moesin may have no additional role in lamellipodial stability. It is formally possible that CALI using MG-labeled 220 does not affect moesin, but given the similar structures of moesin and radixin, we view this as unlikely.

Micro-CALI of Radixin Does Not Affect Neurite Extension

An additional demonstration of the specificity of micro-CALI of radixin was provided by comparing neurite extension rates of neurons, loaded with MG-labeled 457–3, 220, and IgG, before, during, and after

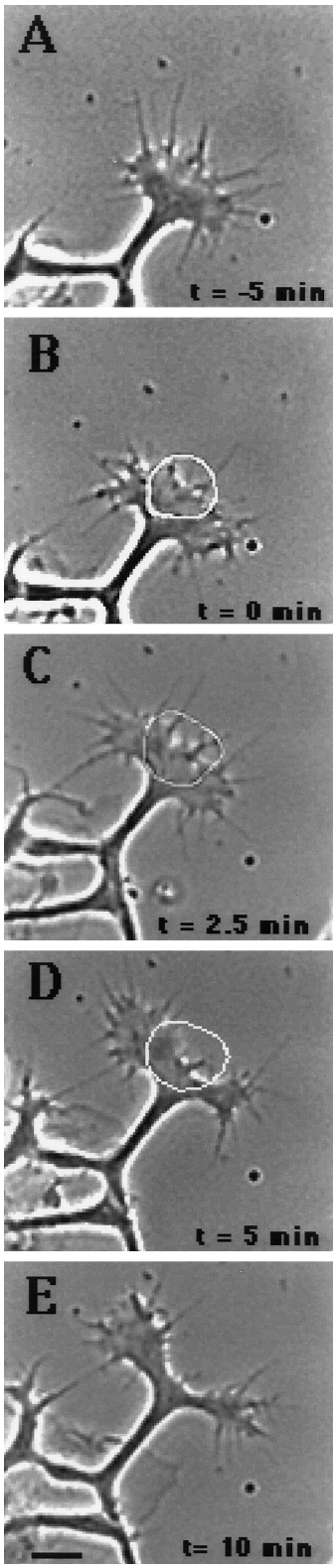

Figure 4. Micro-CALI of radixin in the central region causes growth cone splitting. A chick DRG neuron was loaded with MG-labeled 457–3 and plated on a laminin-coated coverslip to allow a growth cone to emerge. Time-lapse imaging was begun at t = −5 min (A). The growth cone was subjected to laser irradiation in its central region (white circle) beginning at t = 0 min (B) and ending at t = 5 min (C), and the growth cone was observed for another 10 min (D and E). The lamellipodia in the irradiated region retract (B and C), and the growth cone splits into two small growth cones (D and E). Similar results were seen using MG-labeled 220 in place of MG-labeled 457–3 (our unpublished results). No effect was seen with MG-labeled nonimmune IgG (see Table 2). Scale bar, 10 μm.

asymmetric laser irradiation. We also examined the extension rates of neurons loaded with unlabeled 457–3 and 220 (Table 3). Neurite extension rates for all of these treatments (regardless of laser light) were not significantly different than the rate of neurite extension for untreated neurons ($p > 0.15$ for all pairwise comparisons during or after irradiation). These data show that the acute loss of radixin by micro-CALI does not affect neurite extension. They provide evidence that this treatment does not cause nonspecific damage to growth cones that results in their collapse.

DISCUSSION

We have shown that the acute loss of radixin generated by micro-CALI caused lamellipodial retraction within the region of inactivation and growth cone splitting when micro-CALI was targeted to the middle of the leading edge. Growth cones are held under tension as they move (Bray, 1979), and this tension is important for subsequent neurite outgrowth (Bray, 1984). Letourneau *et al.* (1986) proposed that a critical step in branching is the spreading of the neurite cytoskeleton by tension generated at the lateral margins of the leading edge of the growth cone. Our findings are consistent with radixin maintaining the stability of lamellipodia that resists this tension. When radixin's function is diminished at the leading edge, this may cause a local weakening of the cytoskeleton in the irradiated region. Subsequent movement splits the growth cone at this site to generate branching into two new growth cones. As such, a localized change in radixin function at the leading edge can affect the pattern of neurite outgrowth.

The Effects of Micro-CALI of Radixin Are Specific

The effects of micro-CALI of radixin on lamellipodia were not likely due to nonspecific damage of the cytoskeleton. Micro-CALI of radixin using antibodies that recognize different domains of radixin had similar effects. CALI-induced damage is spatially restricted with a half-maximal radius of damage of 15 Å around each dye moeity (Liao *et al.*, 1994). This approach has been used to inactivate single subunits in the T cell receptor with only slight effects on nearest neighbors in the complex (Liao *et al.*, 1995). CALI is spatially

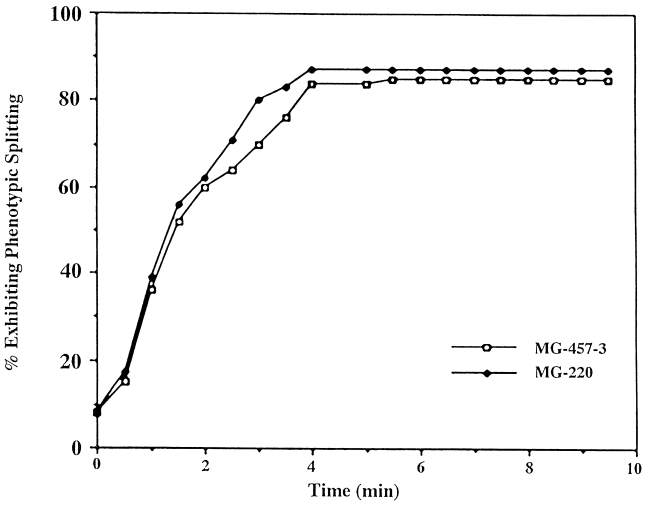

Figure 5. The effects of micro-CALI of radixin and of all ERMs are indistinguishable. The time course for growth cone splitting was plotted for all samples subjected to micro-CALI of radixin alone and micro-CALI of all ERMs. Growth cone splitting is initiated early during laser irradiation and occurs rapidly for both treatments.

restricted even between different domains of a single protein. For example, CALI using an antibody that recognizes the tail and neck domain of myosin V inhibits in vitro motility associated with the neck domain without affecting the actin-dependent ATPase activity associated with the head domain (Wang *et al.*, 1996). CALI has mimicked genetic loss of function in *Drosophila* in all cases tested directly (Schmucker *et al.*, 1994; Schroeder *et al.*, 1996). Micro-CALI performed on a variety of actin-associated proteins in nerve growth cones has shown distinct effects on motility for each protein studied (Sydor *et al.*, 1996; Wang *et al.*, 1996). For example, micro-CALI of myosin Iβ caused lamellipodial expansion into the laser spot (Wang *et al.*, 1996). Finally, micro-CALI targeted directly to actin in growth cones using MG-labeled G-actin had no effect on motility (Sydor, 1995). Although it not possible to entirely rule out that CALI damages neighboring proteins for any specific case, these studies suggest that this is unlikely to occur.

Radixin and Ezrin May Play Similar Roles in Different Cell Types

A recent study using micro-CALI of ezrin (Lamb *et al.*, 1997) showed a role for ezrin at the leading edge of transformed fibroblasts. This caused pseudopodial retraction that was similar to the lamellipodial retraction that we observed during micro-CALI of radixin.

This suggests that radixin and ezrin play similar roles in different cell types to stabilize the leading edge of moving cells. However, when ezrin was inactivated in normal fibroblasts, there was a marked and rapid retraction of the entire leading edge when micro-CALI was targeted here. This retraction left fibers remaining on the substrate like those seen on the trailing edge of moving fibroblasts or when these cells detach (Harris, 1994). This difference may be due to the fact that the traction forces that hold cells to the substratum are much stronger for normal fibroblasts (2×10^{-7} N; Harris *et al.*, 1980; Oliver *et al.*, 1995) than for growth cones ($< 6 \times 10^{-9}$ N; Lamoureux *et al.*, 1989).

It has been suggested that radixin and ezrin have redundant function and are coexpressed in many cell types as a safety measure (Tsukita *et al.*, 1997). Our studies support this hypothesis. This may explain why it was necessary to suppress all three ERM proteins in cultured epithelial cells to affect cell attachment (Takeuchi *et al.*, 1994). Chick DRG neurons do not express ezrin (Figure 1A), and thus the effects of the loss of radixin may be more pronounced in neurons compared with other cells. Alternatively, the differ-

Table 2. Micro-CALI of radixin causes growth cone splitting

Treatment	% Of growth cones that split
MG-457-3 (n = 25)	84[a]
MG-220 (n = 23)	87[a]
MG-IgG (n = 22)	5
457-3 (no MG) (n = 20)	0
220 (no MG) (n = 20)	0
Untreated (n = 11)	0

Micro-CALI of radixin using MG-457-3 or MG-220 causes growth cone splitting. Splitting is defined as the retraction of lamellipodia of the central region of the growth cone followed by the formation of two distinct growth cones.

[a] Significance was determined by the Poisson test, $p < 0.0001$.

Table 3. Micro-CALI of radixin does not affect neurite extension

	Rates of change of neurite length (μm/min)		
Treatment	Prelaser	During laser	Postlaser
MG-457-3 (n = 25)	0.5 ± 1.2	0.9 ± 1.8	1.2 ± 2.4
MG-220 (n = 23)	0.4 ± 0.9	1.2 ± 3.5	0.8 ± 0.9
MG-IgG (n = 22)	0.3 ± 1.9	0.8 ± 0.8	0.6 ± 1.4
457-3 (no MG) (n = 20)	0.2 ± 1.5	0.7 ± 1.3	1.2 ± 0.5
220 (no MG) (n = 20)	0.5 ± 0.9	1.6 ± 2.3	0.2 ± 1.7
Untreated (n = 11)	0.7 ± 1.3	0.8 ± 1.1	1.0 ± 0.7

Micro-CALI of radixin does not affect neurite extension. No significant difference was observed between all treatment samples.

ence in severity observed here compared with antisense experiments may be due to the nature of disruption of the two methods. Antisense RNA generates the chronic and global loss of cellular expression of any particular protein. It may allow compensation of proteins with overlapping function although no increase in expression was observed in these antisense experiments (Takeuchi *et al.*, 1994). Micro-CALI allowed us to observe localized changes in motility and growth cone shape during inactivation. This analysis likely precludes compensation. Thus, micro-CALI provides a good test of a protein's function during motility.

Radixin's Role in Lamellipodia

Our findings show that radixin is involved in lamellipodial stability but do not demonstrate how radixin acts here. Cells must regulate the connections of the cytoskeletal network to effect cell shape changes during motility (Ingber *et al.*, 1994). These connections may be maintained to resist tensile force or may give way to change cell shape (Mooney *et al.*, 1995). Radixin is a good candidate to play this role in nerve growth cones because it is found in growth cones (Gonzalez-Agosti and Solomon, 1996) and has in vitro binding sites for F-actin (Algrain *et al.*, 1993; Henry *et al.*, 1995) and membrane proteins (Tsukita *et al.*, 1994). It has been suggested that radixin may cross-link actin filaments or link F-actin to the plasma membrane (Algrain *et al.*, 1993; Tsukita *et al.*, 1994, 1997), and our findings are consistent with this notion. ERM binding to F-actin and membranes may be regulated by signal transduction (Bretscher, 1989; Nakamura *et al.*, 1995; Hirao *et al.*, 1996; MacKay *et al.* 1997; Potter *et al.*, 1998). As such, radixin may act to translate signals from extracellular cues to change shape and motility at the growth cone's leading edge.

Radixin may also function in actin assembly by its barbed end capping activity (Tsukita *et al.*, 1989). Our observations would be consistent with a loss of actin assembly at the leading edge causing localized lamellipodial retraction. Micro-CALI of radixin could modify radixin such that F-actin at the leading edge could not be uncapped. A loss in adhesion at the leading edge could also cause lamellipodial retraction, and it has also been suggested that ERM proteins may have a role in cell adhesion (Takeuchi *et al.*, 1994; MacKay *et al.*, 1997). Establishing which of these cellular processes are critical for radixin's action in lamellipodia will require a detailed analysis of ultrastuctural changes in F-actin in response to micro-CALI of radixin.

ACKNOWLEDGMENTS

The authors are very grateful to Alian Xu for technical assistance, to Frank Solomon and Etchell Cordero (MIT, Cambridge MA) for generous gifts of antibodies and helpful discussions. We also thank Elizabeth Luna (University of Massachusetts, Worchester, MA) for helpful discussion and to Ira Herman, Arthur Lander, and members of our laboratory for critical reading of the manuscript. This work was supported by a grant to D.G.J. from the National Institutes of Health (NS-34699-03) and by a National Aeronautics and Space Administration undergraduate fellowship to L.C.

REFERENCES

Algrain, M., Turunen, O., Vaheri, A., Louvard, D., and Arpin, M. (1993). Ezrin contains cytoskeletal and membrane binding domains accounting for its proposed role as a membrane-cytoskeletal linker. J. Cell Biol. *120*, 129–139.

Arpin, M., Algrain, M., and Louvard, D. (1994). Membrane-actin microfilament connection: an increasing diversity of players related to band 4.1. Curr. Opin. Cell Biol. *6*, 136–141.

Beerman, A.E., and Jay, D.G. (1994). Chromophore-assisted laser inactivation of cellular proteins. Methods Cell Biol. *44*, 716–732.

Bentley, D., and Toroian-Raymond, A. (1986). Disoriented pathfinding by pioneer neuron growth cones deprived of filopodia by cytochalasin treatment. Nature *323*, 712–715.

Birgbauer, E., Dinsmore, J.H., Winckler, B., Lander, A.D., and Solomon, F. (1991). Association of ezrin isoforms with the neuronal cytoskeleton. J. Neurosci. Res. *30*, 232–241.

Borasio, G.D., John, J., Wittinghofer, A., Barde, Y.A., Sendtner, M., and Heurmann, R. (1989). ras p21 protein promotes survival and fiber outgrowth of cultured embryonic neurons. Neuron *2*, 1087–1096.

Bray, D. (1979). Mechanical tension produced by nerve cells in tissue culture. J. Cell Sci. *37*, 391–410.

Bray, D. (1984). Axonal growth in response to experimentally applied mechanical tension. Dev. Biol. *102*, 379–389.

Bretscher, A. (1989). Rapid phosphorylation and reorganization of ezrin and spectrin accompany morphological changes induced in A-431 cells by epidermal growth factor. J. Cell Biol. *108*, 921–930.

Chang, H., Takei, K., Sydor, A., Born, T., Rusnak, F., and Jay, D.G. (1995). Asymmetric retraction of growth cone filopodia following focal inactivation of calcineurin. Nature *376*, 686–690.

Diamond, P., Mallavarapu, A., Schnipper, J., Booth, J., Park, L., O'Connor, T.P., and Jay, D.G. (1993). Fasciclin I and II have distinct roles in the development of grasshopper pioneer neurons. Neuron *11*, 409–421.

Dubreil, R., Byers, T.J., Branton, D., Goldstein, L.S.B., and Keihart, D.P. (1987). *Drosophila* spectrin I. Characterization of the purified protein. J. Cell Biol. *105*, 2095–2102.

Everett, A.W., and Nichol, K.A. (1990). Ezrin immunoreactivity in neuronal subpopulations: cellular distribution in relation to cytoskeletal proteins in sensory neurons. J. Histochem. Cytochem. *38*, 1137–1144.

Funayama, N., Nagafuchi, A., Sato, N., Tsukita, Sa., and Tsukita, Sh. (1991). Radixin is a novel member of the band 4.1 family. J. Cell Biol. *115*, 1039–1048.

Gary, R., and Bretscher, A. (1993). Heterotypic and homotypic associations between ezrin and moesin, two putative membrane-cytoskeletal linking proteins. Proc. Natl. Acad. Sci. USA *90*, 10846–10850.

Gonzalez-Agosti, C., and Solomon, F. (1996). Response of radixin to perturbations of growth cone morphology and motility in chick sympathetic neurons. In Vitro Cell Motil. Cytoskeleton *34*, 122–136.

Goslin, K., Birgbauer, E., Banker, G., and Solomon, F. (1989). The role of the cytoskeleton in organizing growth cones: a microfilament-associated growth cone component depends upon microtubules for its localization. J. Cell Biol. *109*, 1621–1631.

Harris, A.K., Wild, P., and Stopak, D. (1980). Silicon rubber substrata: a new wrinkle in the study of cell locomotion. Science *208*, 177–179.

Henry, M.D., Gonzalez-Agosti, C., and Solomon, F. (1995). Molecular dissection of radixin: distinct and interdependent functions of the amino- and carboxyl-terminal domains. J. Cell Biol. *129*, 1007–1022.

Hirao, M., Sato, N., Kondo, T., Yonemura, S., Monden, M., Sasaki, T., Takai, Y., Tsukita, S., Tsukita, Sh. (1996). Regulation of mechanism of ERM (ezrin/radixin/moesin) protein/plasma membrane association: possible involvement of phosphatidylinositol turnover and rho-dependent signaling pathway. J. Cell Biol. *135*, 37–51.

Ingber, D.E., *et al.* Cellular tensegrity: exploring how mechanical changes in the cytoskeleton regulate cell growth, migration, and tissue pattern during morphogenesis. Int. Rev. Cytol. *150*, 173–224.

Jay, D.G. (1988). Selective destruction of protein function by chromophore-assisted laser inactivation. Proc. Natl. Acad. Sci. USA *85*, 5454–5458.

Jay, D.G. (1996). Molecular mechanisms of directed growth cone motility. Perspect. Dev. Neurobiol. *4*, 137–146.

Lamb R.F., Ozanne, B.W., Roy, C., McGarry, L., Stipp, C., Mangeat, P., and Jay, D.G. (1997). Essential functions of ezrin in maintenance of cell shape and lamellipodial extension in normal and fibroblast transformation. Curr. Biol. *7*, 682–688.

Lamoureux, P., Buxbaum, R.E., and Heidemann, S.R. (1989). Direct evidence that growth cones pull. Nature *340*, 159–162.

Letourneau, P.C. (1996). The cytoskeleton in nerve growth cone motility and axonal pathfinding. Perspect. Dev. Neurobiol. *4*, 111–124.

Letourneau P.C., Shattuck, T.A., and Ressler, A.H. (1986). Branching of sensory and sympathetic neurites in vitro is inhibited by treatment with taxol. J. Neurosci. *6*, 1912–1917.

Liao, J.C., Berg, L.J., and Jay, D.G. (1995). Chromophore-assisted laser inactivation of subunits of the T cell receptor in living cells is spatially restricted. Photochem. Photobiol. *62*, 923–929.

Liao, J.C., Roider, J., and Jay, D.G. (1994). Chromophore-assisted laser inactivation of proteins is mediated by the photogeneration of free radicals. Proc. Natl. Acad. Sci. USA *91*, 2659–2663.

MacKay, D.J.G., Esch, F., Furthmayr, H., and Hall, A. (1997). Rho- and Rac-dependent assembly of focal adhesion complexes and actin filaments in permeabilized fibroblasts: an essential role for ezrin/radixin/moesin proteins. J. Cell Biol. *138*, 927–938.

Magendantz, M., Henry, M., Lander, A., and Solomon, F. (1995). Interdomain interactions of radixin in vitro. J. Biol. Chem. *270*, 25324–25327.

Marsh, L., and Letourneau, P.C. (1984). Growth of neurites without filopodial and lamellipodial activity in the presence of cytochalasin B. J. Cell Biol. *99*, 2041–2047.

Martin, M., Andreoli, C., Sahuquet, A., Montcourrier, P., Algrain, M., and Mangeat, P. (1995). Ezrin NH2-terminal inhibits the cell extension of the COOH-terminal domain. J. Cell Biol. *128*, 1081–1093.

Mooney, D., Langer, R., and Ingber, D. (1995). Cytoskeletal filament assembly and the control of cell spreading and function by extracellular matrix. J. Cell Sci. *108*, 2311–2320.

Nakamura, F., Amieva, M.R., and Furthmayr, H. (1995). Phosphorylation of threonine 558 in the carboxyl-terminal actin binding domain of moesin by thrombin activation of human platelets. J. Biol. Chem. *270*, 31377–31385.

Oliver, T., Dembo, M., and Jacobson, K. (1995). Traction forces in locomoting cells. Cell Motil. Cytoskeleton *31*, 225–240.

Potter, D.A., Tirnauer, J.S., Janssen, R., Croall, D.E., Hughes, C.N., Mier, J.M., Maki, M., and Herman, I.M. (1998). Calpain regulates actin dynamics during cell spreading. J. Cell Biol. *141*, 647–663.

Sato, N., Funayama, N., Nagafuchi, A., Tsukita, Sa., and Tsukita, Sh. (1991). A gene family consisting of ezrin, radixin and moesin. J. Cell Sci. *103*, 1–13.

Schmucker, D., Su, A., Beermann, A., Jackle, H., and Jay, D.G. (1994). Chromophore-assisted laser inactivation of patched protein switches cell fate in the larval visual system of *Drosophila*. Proc. Natl. Acad. Sci. USA. *91*, 2664–26648.

Schroeder, R., Tautz, D., and Jay, D.G. (1996). Chromophore assisted laser inactivation of even skipped in *Drosophila* phenocopies genetic loss of function. Dev. Genes Evol. *206*, 86–88.

Sydor, A.M. (1995). The Role of Cytoskeletal Proteins Talin and Vinculin in Neuronal Growth Cone Motility. Ph.D. Dissertation. Boston MA: The Program in Neuroscience, Harvard Medical School.

Sydor, A.M., Su, A.L., Wang, F., Xu, A., and Jay, D.G. (1996). Talin and vinculin play distinct roles in filopodial motility in the neuronal growth cone. J. Cell Biol. *134*, 1197–1207.

Takeuchi, K., Sato, N., Kasahara, H., Funayama, N., Nagafuchi, A., Yonemura, S., Tsukita, S., and Tsukita, Sh. (1994). Perturbation of cell adhesion and microvilli formation by antisense oligonucleotides to ERM family members. J. Cell Biol. *125*, 1371–1384.

Tanaka, E., and Sabry, J. (1995). Making the connection: cytoskeletal rearrangements during growth cone guidance. Cell *83*, 171–176.

Tsukita, S., Hieda, Y., and Tsukita, Sh. (1989). A new 82-kDa barbed end-capping protein (radixin) localized in the cell-to-cell adherens junction: purification and characterization. J. Cell Biol. *108*, 269–2382.

Tsukita, S., Oishi, K., Sato, N., Sagara, J., Kawai, A., and Tsukita, S. (1994). ERM family members as molecular linkers between the cell surface glycoprotein CD44 and actin-based cytoskeleton. J. Cell Biol. *126*, 391–401.

Tsukita, S., Yonemura, S., and Tsukita, S. (1997). ERM (ezrin/radixin/moesin) family: from cytoskeleton to signal transduction. Curr. Opin. Cell Biol. *9*, 70–75.

Turunen, O., Wahlstrom, T., and Vaheri, A. (1994). Ezrin has a COOH-terminal actin binding site that is conserved in the ezrin protein family. J. Cell Biol. *126*, 1445–1453.

Wang, F.S., and Jay, D.G. (1996). Chromophore-assisted laser inactivation (CALI): probing protein function in situ with a high degree of spatial and temporal resolution. Trends Cell Biol. *6*, 442–445.

Wang, F.S., Wolenski, J.S., Cheney, R.E., Mooseker, M.S., and Jay, D.G. (1996). Function of myosin-V in filopodial extension of neuronal growth cones. Science *273*, 660–663.

Winckler, B., Gonzalez-Agosti, C., Magendantz, M., and Solomon, F. (1994). Analysis of a cortical cytoskeletal structure: a role for ezrin-radixin-moesin (ERM proteins) in the marginal band of chicken erythrocytes. J. Cell Sci. *107*, 2523–2534.